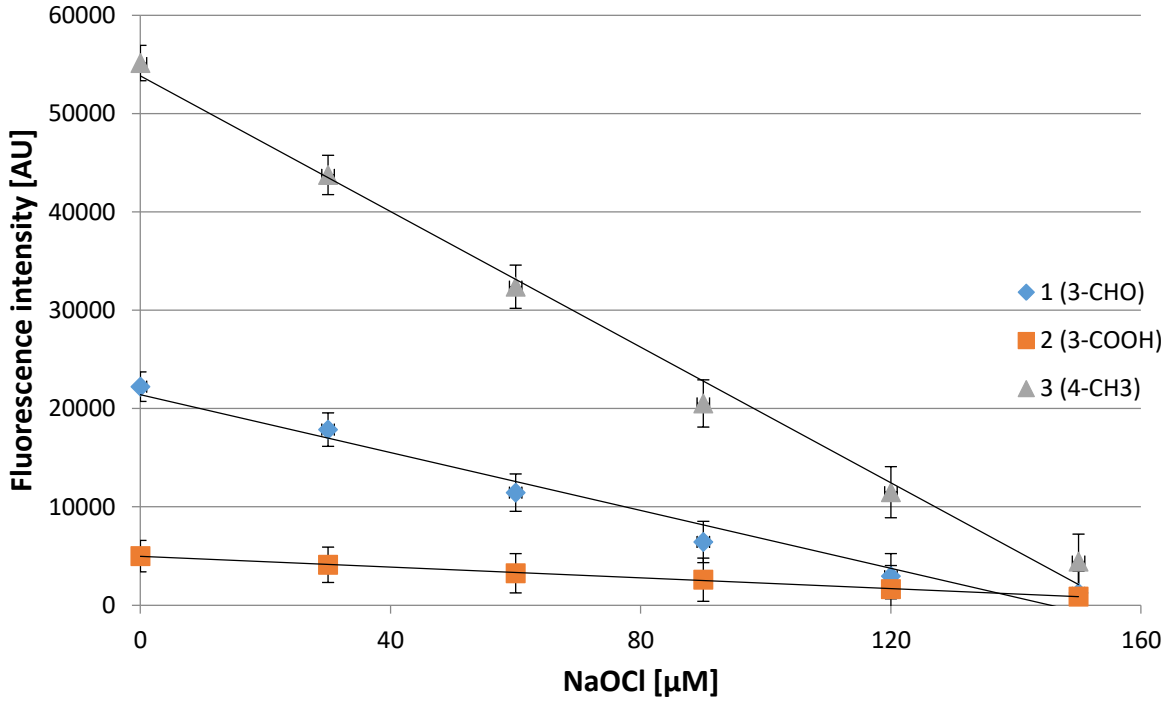


Figure 1S. Changes in fluorescence intensity of **1- 3** induced by an increase in NaOCl concentration, at pH 3, $\lambda_{Ex}$ 289 nm, and the temperature of 25 °C.

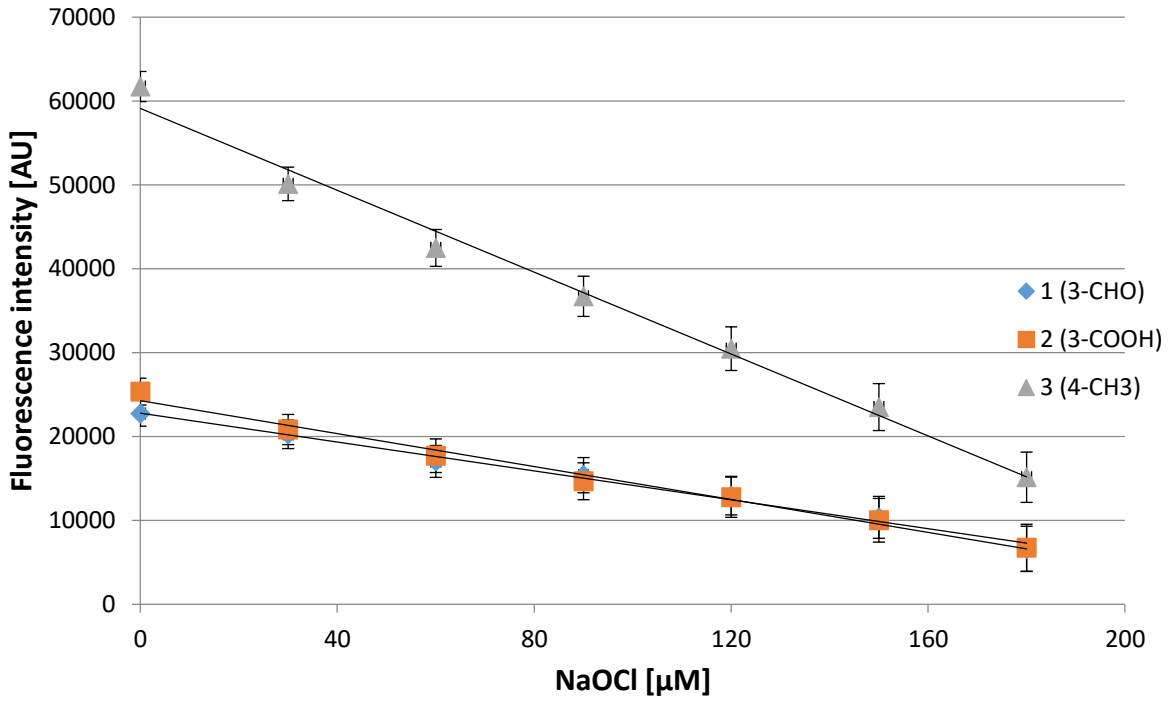


Figure 2S. Changes in fluorescence intensity of **1- 3** induced by an increase in NaOCl concentration, at pH 7.4, $\lambda_{Ex}$ 289 nm, and the temperature of 25 °C.

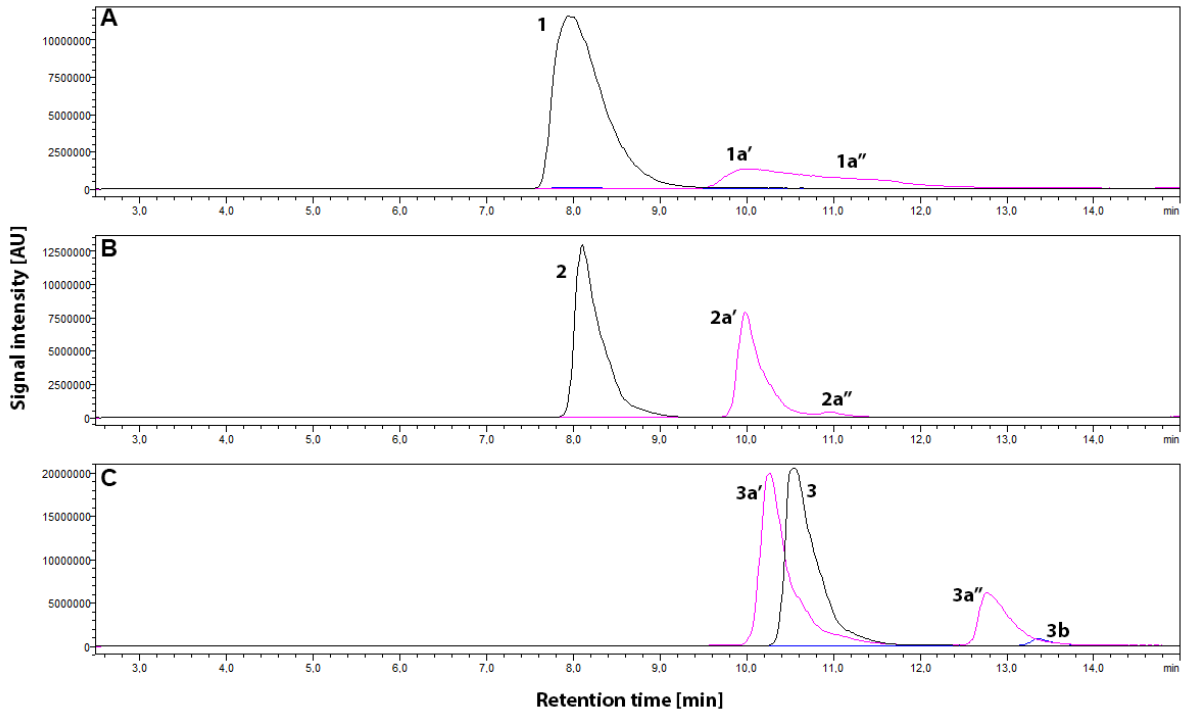


Figure 3S. HPLC-MS traces of chlorination products of 150 μM probes **1** (A), **2** (B), **3** (C) by 150 μM NaOCl at pH 5 and the temperature of 25 °C. Peak numbering is presented in Table 1.

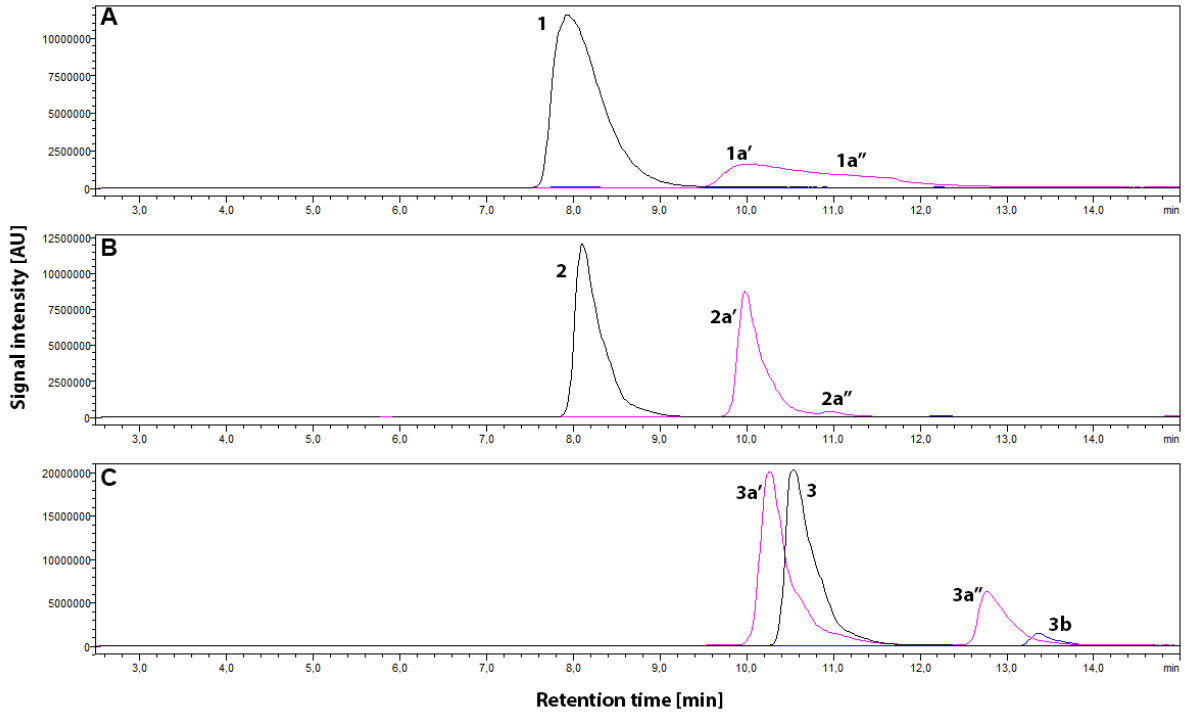


Figure 4S. HPLC-MS traces of chlorination products of 150 μM probes **1** (A), **2** (B), **3** (C) by 150 μM NaOCl at pH 7.4 and the temperature of 25 °C. Peak numbering is presented in Table 1.

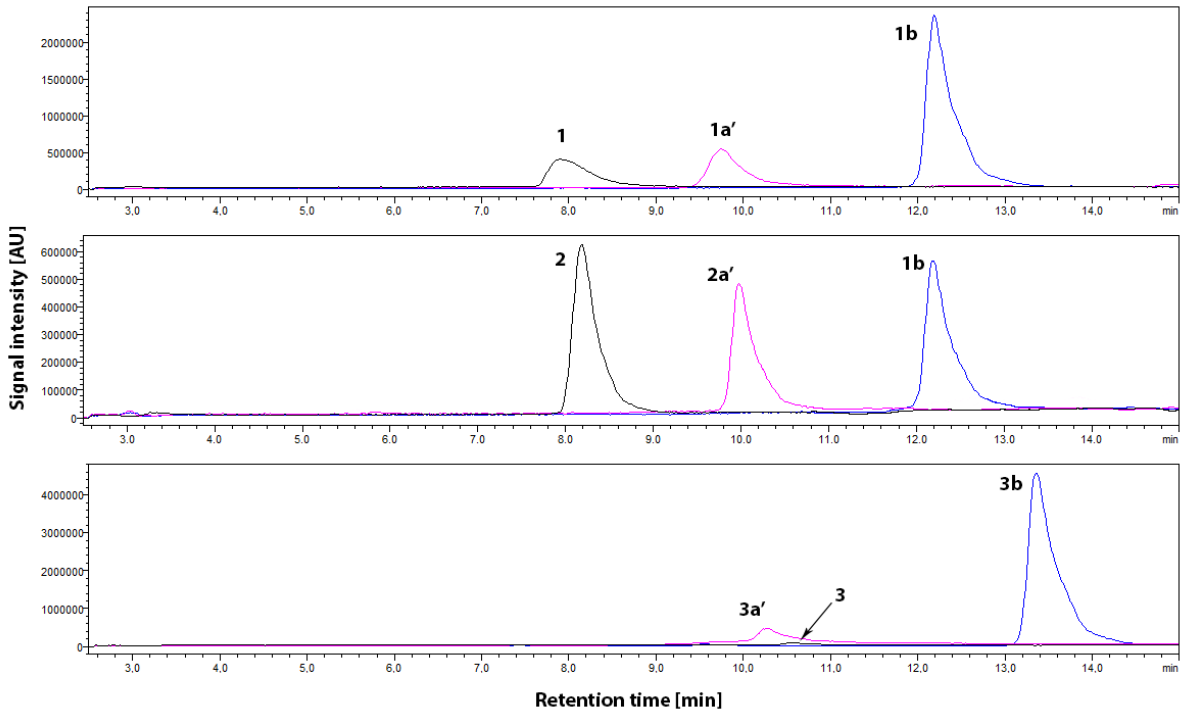


Figure 5S. HPLC-MS traces of chlorination products of 150 μM probes **1-3** by 5-fold excess NaOCl at pH 3 and the temperature of 25 °C. Peak numbering is presented in Table 1S.

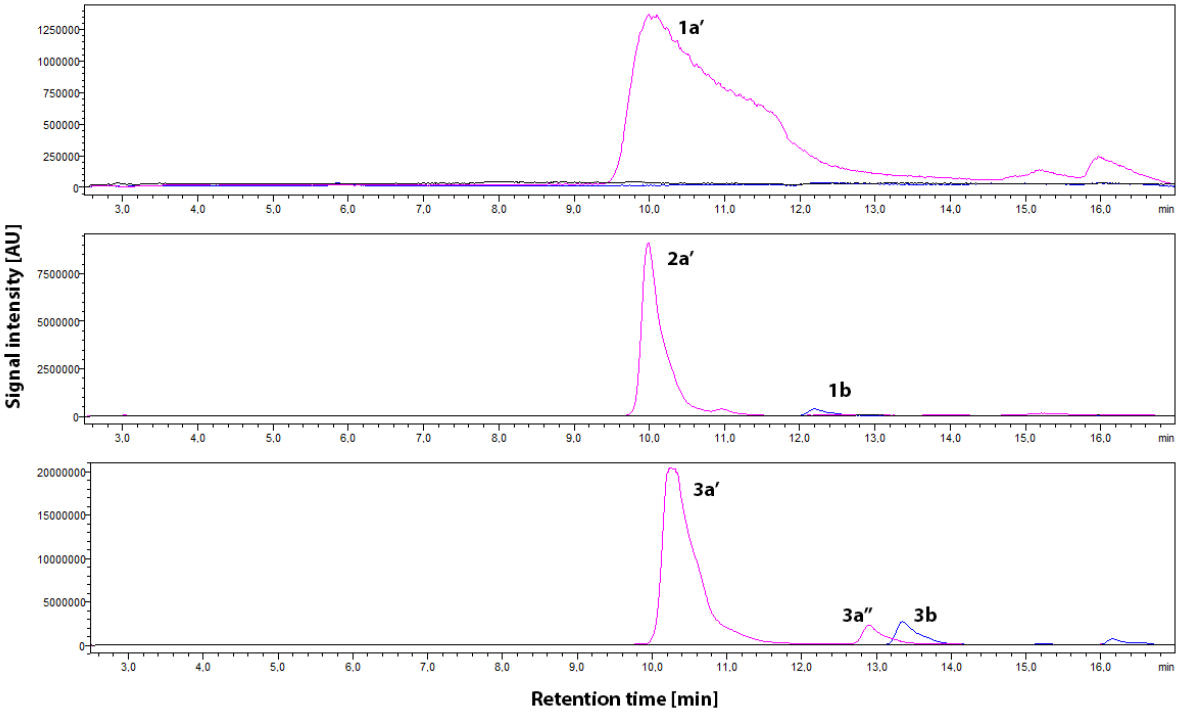


Figure 6S. HPLC-MS traces of chlorination products of 150 μM probes **1-3** by 5-fold excess NaOCl at pH 5 and the temperature of 25 °C. Peak numbering is presented in Table 1S.

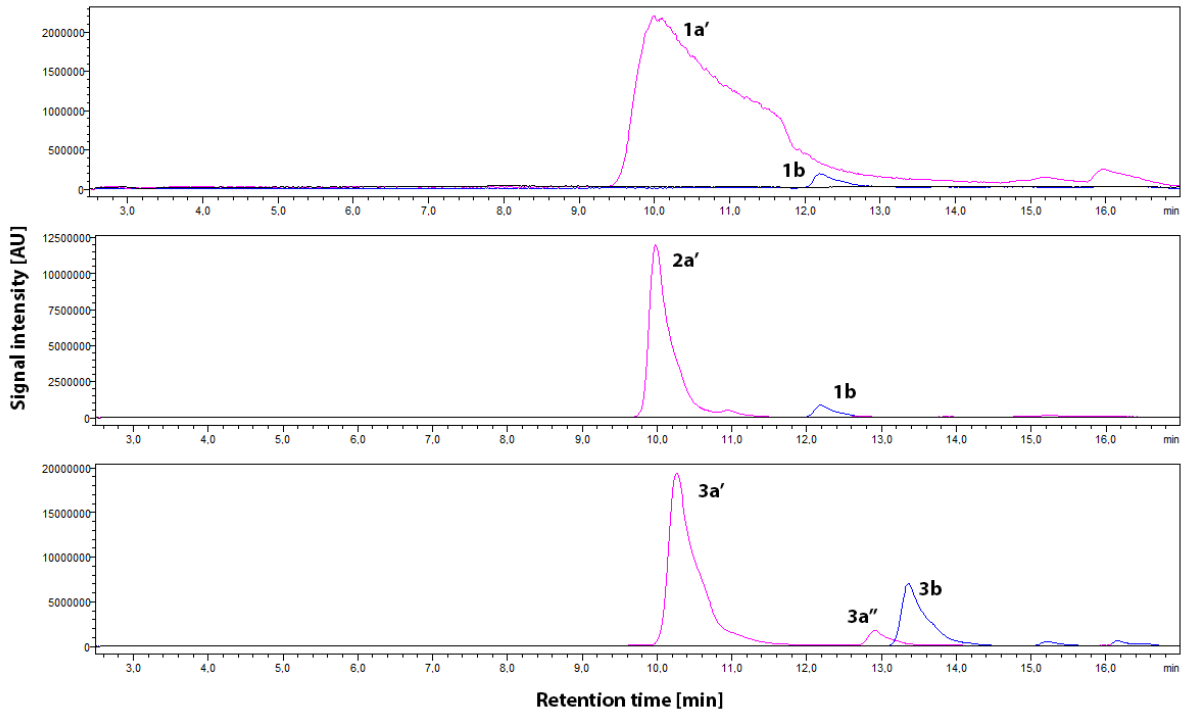


Figure 7S. HPLC-MS traces of chlorination products of 150 µM probes **1-3** by 5-fold excess NaOCl at pH 7.4 and the temperature of 25 °C. Peak numbering is presented in Table 1S.

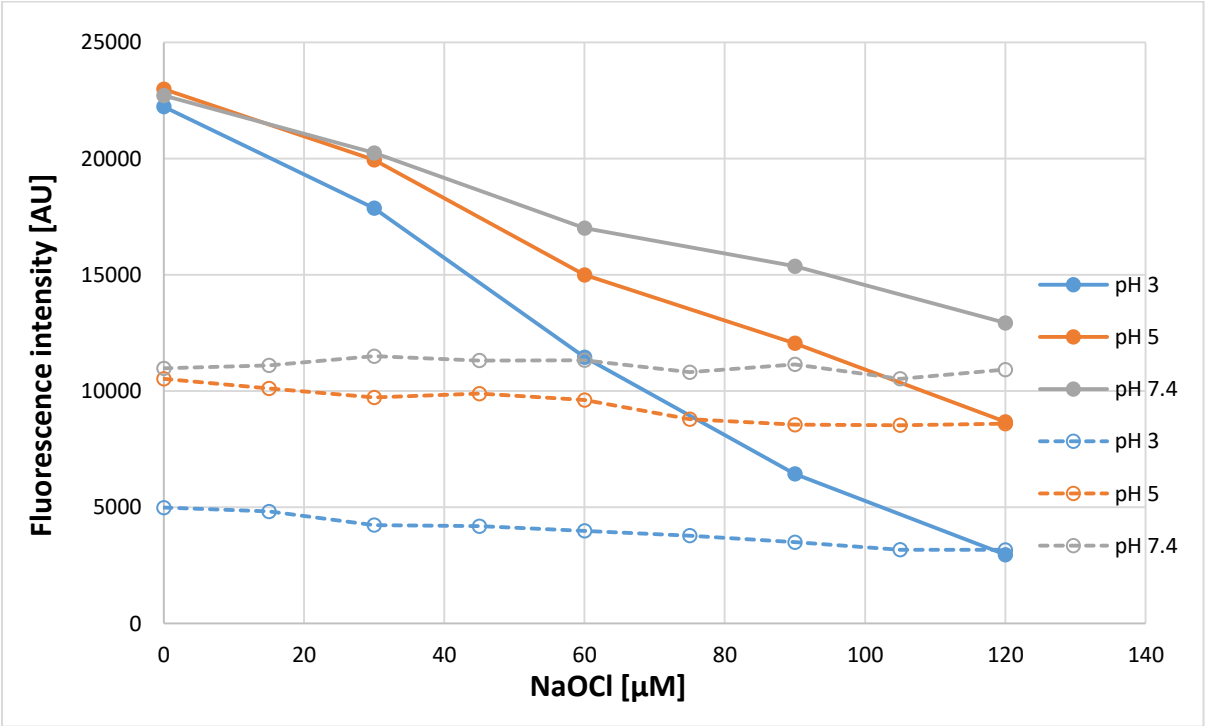


Figure 8S. Comparison of sodium hypochlorite-induced changes in fluorescence intensity of **1** (150 µM) (permanent lines), with that recorded upon the addition of Trolox (40 µM) (dashed lines). The measurements were carried out at $\lambda_{Ex}$ 289 nm, $\lambda_{Em}$ 464 nm, and a temperature of 25 °C.

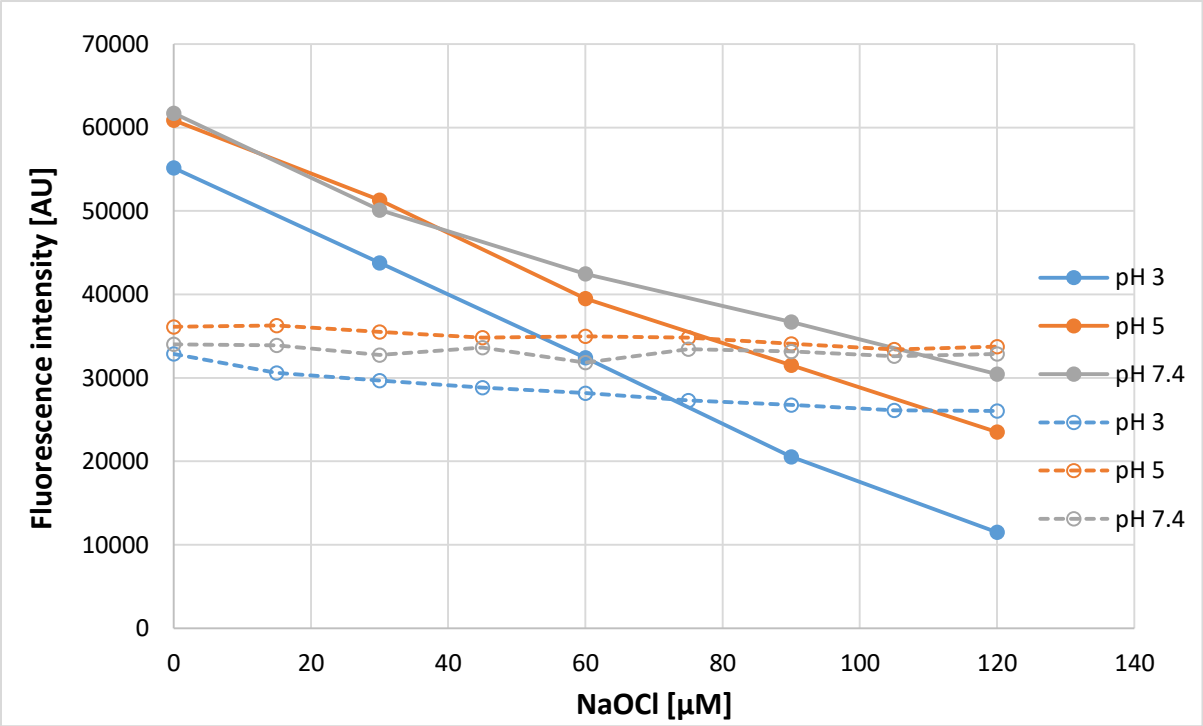


Figure 9S. Comparison of sodium hypochlorite-induced changes in fluorescence intensity of **3** (150 µM) (permanent lines), with that recorded upon the addition of Trolox (40 µM) (dashed lines). The measurements were carried out at $\lambda_{Ex}$ 289 nm, $\lambda_{Em}$ 450 nm, and a temperature of 25 °C.

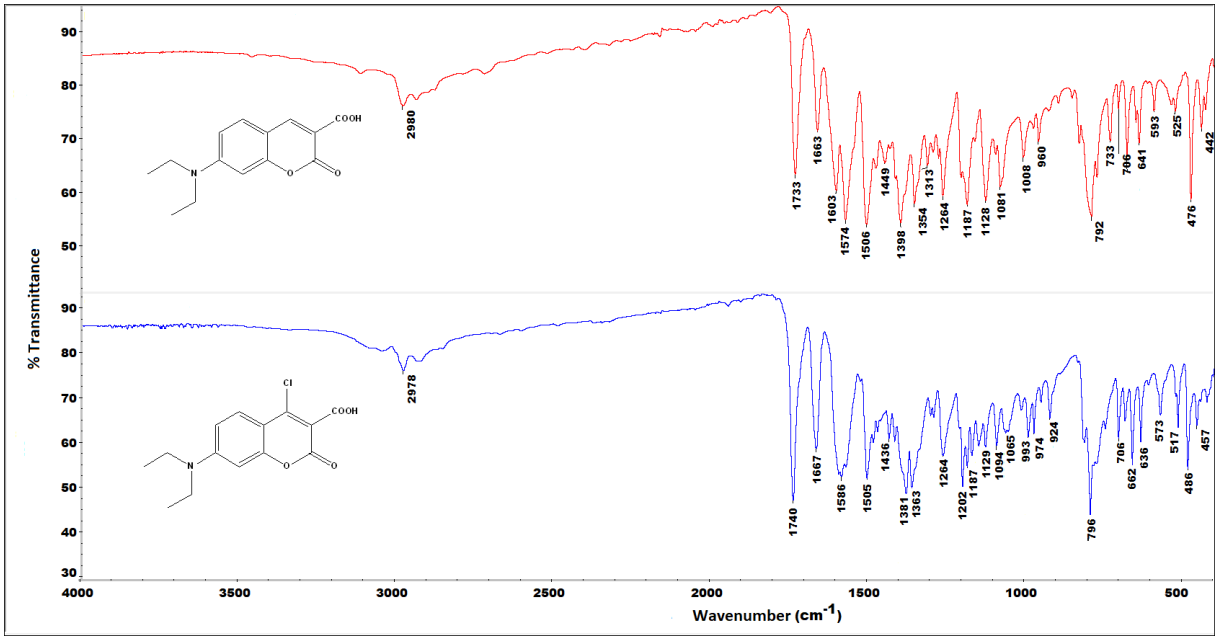


Figure 10S. Comparison of IR(ATR) Spectra of **2** (upper) and its corresponding chlorinated derivative **2a'** (bottom)

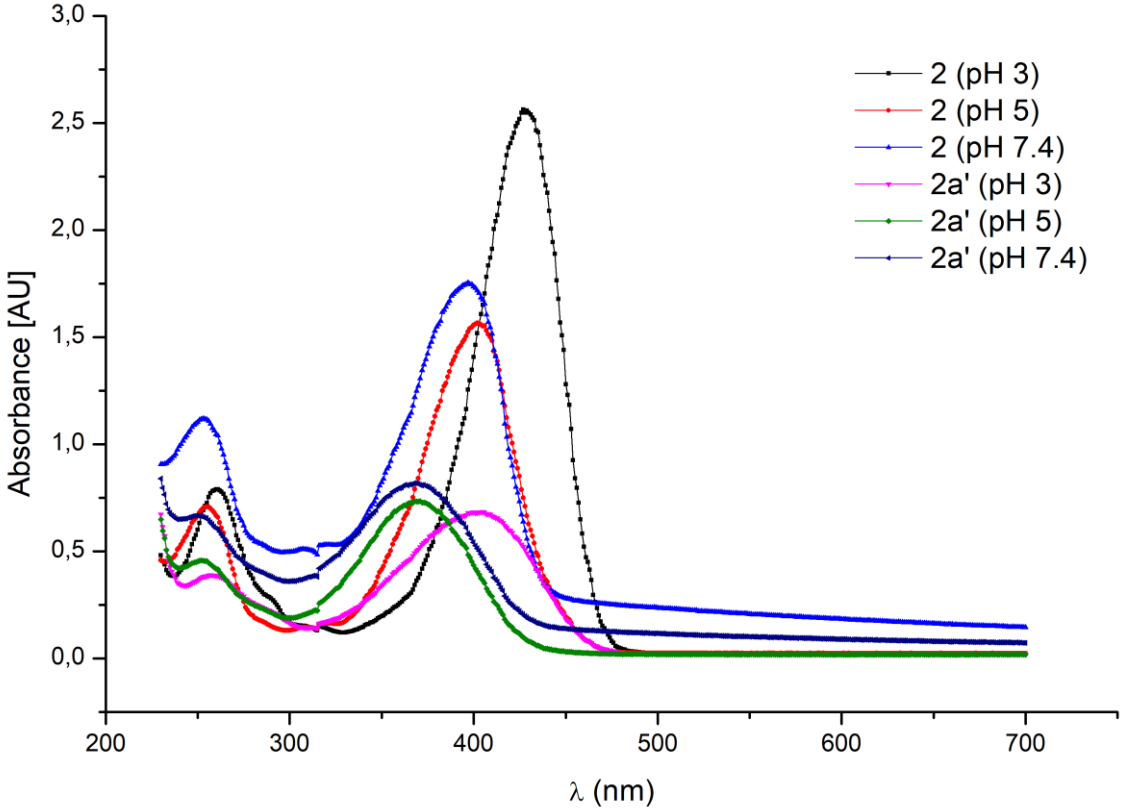


Figure 11S. UV-Vis absorption spectra of the isolated derivative **2a'** and its respective substrate **2** recorded at conditions identical to those applied for the hypochlorite sensing experiment (concentration of 150 uM, various pH, $\lambda_{Ex}$=289, and the temperature of 25 °C).

Table 1S. Chromatographic, spectrophotometric, and mass spectrometric data for the coumarin derivatives **1-3** and their corresponding chlorinated products at pH 3 after 15 minutes of reaction with fivefold excess of hypochlorite.

| Compound No. | Compound name | $t_{ret}$ [min] | $\lambda_{max}$ [nm] | *m/z* $[M+H]^+$ | Composition [%] |
|---|---|---|---|---|---|
| **1** | 7-diethylamino-3-formylcoumarin | 7.9 | 443 | 246.05 | 1.6 |
| **1a'** | monochloro-7-diethylamino-3-formylcoumarin* | 9.7 | 433 | 279.95 | 2.0 |
| **1b** | dichloro-7-diethylaminocoumarin* | 12.1 | 366 | 285.95 | 8.7 |
| **2** | 7-diethylaminocoumarin-3-carboxylic acid | 8.1 | 432 | 262.00 | 3.0 |
| **2a'** | monochloro-7-diethylaminocoumarin-3-carboxylic acid* | 9.9 | 411 | 295.95 | 2.1 |
| **1b** | dichloro-7-diethylaminocoumarin* | 12.1 | 366 | 285.90 | 2.6 |
| **3a'** | monochloro-7-diethylamino-4-methylcoumarin* | 10.2 | 350 | 266.00 | 0.7 |
| **3** | 7-diethylamino-4-methylcoumarin | 10.5 | 375 | 232.05 | 0.1 |
| **3b** | dichloro-7-diethylamino-4-methylcoumarin* | 13.3 | 360 | 299.95 | 9.8 |